# Stimuli Responsive Systems Constructed Using Cucurbit[*n*]uril-Type Molecular Containers
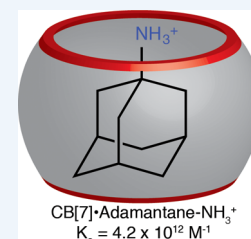
Lyle Isaacs*

Department of Chemistry and Biochemistry, University of Maryland, College Park, Maryland 20742, United States

**CONSPECTUS:** This Account focuses on stimuli responsive systems that function in aqueous solution using examples drawn from the work of the Isaacs group using cucurbit[*n*]uril (CB[*n*]) molecular containers as key recognition elements. Our entry into the area of stimuli responsive systems began with the preparation of glycoluril derived molecular clips that efficiently distinguish between self and nonself by H-bonds and $\pi-\pi$ interactions even within complex mixtures and therefore undergo self-sorting. We concluded that the selectivity of a wide variety of H-bonded supramolecular assemblies was higher than previously appreciated and that self-sorting is not exceptional behavior. This lead us to examine self-sorting within the context of CB[*n*] host–guest chemistry in water.



CB[7]·Adamantane-NH$_3^+$
$K_a = 4.2 \times 10^{12}$ M$^{-1}$

We discovered that CB[*n*] homologues (CB[7] and CB[8]) display remarkably high binding affinity ($K_a$ up to $10^{17}$ M$^{-1}$) and selectivity ($\Delta\Delta G$) toward their guests, which renders CB[*n*]s prime components for the construction of stimuli responsive host–guest systems. The CB[7]·adamantaneammonium ion complex, which is particularly privileged ($K_a = 4.2 \times 10^{12}$ M$^{-1}$), was introduced by us as a stimulus to trigger constitutional changes in multicomponent self-sorting systems. For example, we describe how the free energy associated with the formation of host–guest complexes of CB[*n*]-type receptors can drive conformational changes of included guests like triazene–arylene foldamers and cationic calix[4]arenes, as well as induced conformational changes (e.g., ammonium guest size dependent homotropic allostery, metal ion triggered folding, and heterochiral dimerization) of the hosts themselves.
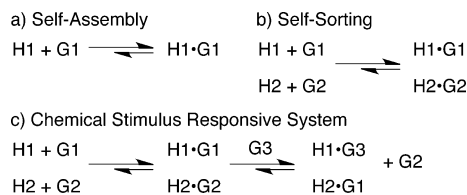
Many guests display large p$K_a$ shifts within their CB[*n*]–guest complexes, which we used to promote pH controlled guest swapping and thermal *trans*-to-*cis* isomerization of azobenzene derivatives. We also used the high affinity and selectivity of CB[7] toward its guests to outcompete an enzyme (bovine carbonic anhydrase) for a two-faced inhibitor, which allowed stimuli responsive regulation of enzymatic activity. These results prompted us to examine the use of CB[*n*]-type receptors in both *in vitro* and *in vivo* biological systems. We demonstrated that adamantaneammonium ion can be used to intracellularly sequester CB[7] from gold nanoparticles passivated with hexanediammonium ion·CB[7] complexes and thereby trigger cytotoxicity. CB[7] derivatives bearing a biotin targeting group enhance the cytotoxicity of encapsulated oxaliplatin toward L1210FR cells. Finally, acyclic CB[*n*]-type receptors function as solubilizing excipients for insoluble drugs for drug delivery purposes and as a broad spectrum reversal agent for the neuromuscular blocking agents rocuronium, vecuronium, and *cis*-atracurium in rats. The work highlights the great potential for integration of CB[*n*]-type receptors with biological systems.

## ■ INTRODUCTION

Herein, I present an Account of research performed in my group directed toward the development of stimuli responsive systems using cucurbit[*n*]uril (CB[*n*]) molecular containers and other glycoluril derived systems as key recognition components. In the 1990s, the supramolecular chemistry field began to use its fundamental knowledge of noncovalent interactions (e.g., H-bonds, metal–ligand interactions, electrostatic interactions, and the solvophobic effect) to enable the preparation of more complex multicomponent aggregates formed in self-assembly processes. For the purpose of this Account, we define self-assembly as those processes that result in the transformation of a set of building blocks into one well-defined aggregate under a specific set of conditions (Scheme 1a). Self-sorting can then be defined as the concurrent self-assembly of multiple sets of building blocks into multiple well-defined aggregates under a specific set of conditions (Scheme 1b). The focus of this Account, stimuli responsive systems, is those self-assembling or self-sorting systems whose constituents can be reconfigured in response to suitable stimuli (e.g., pH

**Scheme 1. Concepts of (a) Self-Assembly, (b) Self-Sorting, and (c) Chemical Stimulus Responsive Systems**



a) Self-Assembly

H1 + G1 ⇌ H1·G1

b) Self-Sorting

H1 + G1 ⇌ H1·G1

H2 + G2 ⇌ H2·G2

c) Chemical Stimulus Responsive System

H1 + G1 ⇌ H1·G1 —G3→ H1·G3 + G2
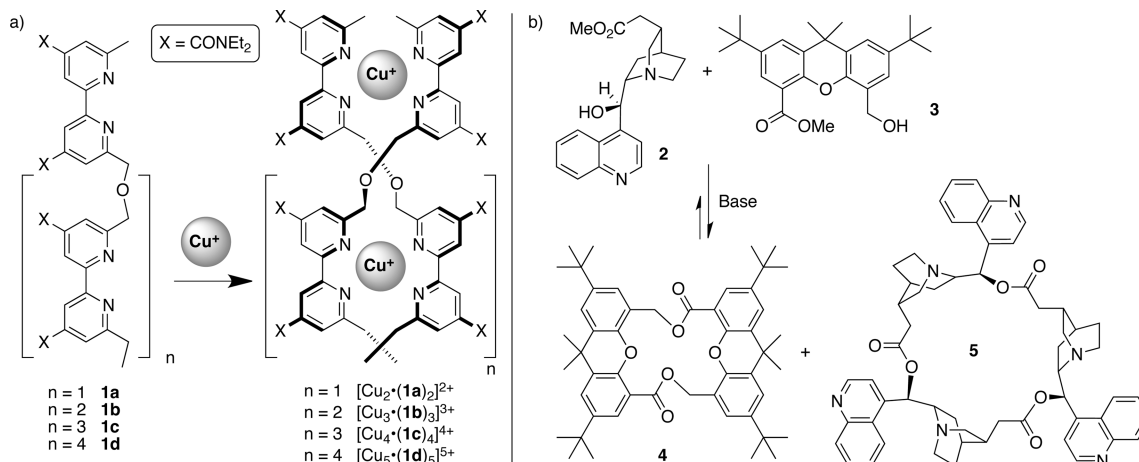
H2 + G2 ⇌ H2·G2        H2·G1

change, photochemistry, electrochemistry, addition of further constituents). In stimulus responsive systems (Scheme 1c), the most potent stimuli are those that result in large favorable changes in the overall free energy ($\Delta\Delta G$) after application of the stimulus that can drive substantial changes in constitution.

**Scheme 2. Self-Sorting Processes**

Lehn conceptualized self-recognition processes in the context of the self-assembly of a series oligo(bipyridine) compounds (**1**) in the presence of Cu⁺ ions (Scheme 2a).[1] Individually, compounds **1a−1d** self-assemble with Cu⁺ to give the double helicates [**1a₂·Cu₂**]²⁺−[**1d₅·Cu₅**]⁵⁺. Remarkably, the mixture of the four structurally similar strands (**1a−d**) and Cu⁺ gives [**1a₂·Cu₂**]²⁺−[**1d₅·Cu₅**]⁵⁺ in a high fidelity self-recognition process. The Sanders group first used the term self-sorting to describe the behavior of a mixture of building blocks (**2 and 3**) under thermodynamically controlled transesterification conditions (Scheme 2b).[2] Interestingly, a mixture of the two homomeric macrocycles **4 and 5** is formed in a high fidelity self-sorting process. In both of these pioneering works, the focus was on self-processes where each compound recognizes other identical building blocks within a mixture.

In this Account, we use glycoluril derived systems whose development can be traced to the early work of Mock, Nolte, and Rebek.[3−5] In 1981, Mock reported that the reaction of glycoluril and formaldehyde under strongly acidic conditions yields cucurbit[6]uril (CB[6]); subsequent work by Kim, Day, and Isaacs using milder reaction conditions produced CB[n] homologues CB[5], CB[7], CB[8], and CB[10] (Figure 1).[6−8]
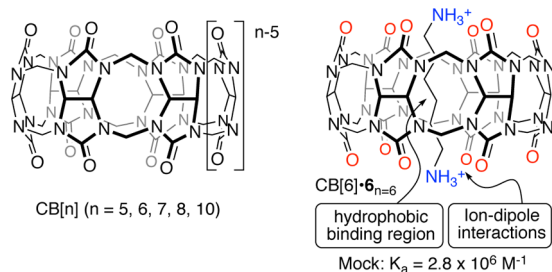


**Figure 1.** Structures of CB[n] and CB[6]·**6**ₙ₌₆ complex.

CB[n] chemistry is the subject of comprehensive reviews.[9] Mock showed that CB[6] shows high affinity toward alkanediammoniums (⁺H₃N(CH₂)ₙNH₃⁺, **6**ₙ) in HCO₂H−water mixtures in a process driven by the hydrophobic effect and ion−dipole interactions between the ammoniums and the two symmetry equivalent C=O portals of CB[n]. CB[6] also displays high selectivity based on length with **6**ₙ₌₅,₆ being preferred.

## SELF-SORTING SYSTEMS BASED ON SELF-RECOGNITION

As part of our synthetic and mechanistic studies toward CB[n]-type receptors[10,11] we prepared molecular clips **7−9**, which feature a central glycoluril dimer framed by aromatic walls that display two H-bonding arms in different three-dimensional arrangements (Figure 2a).[12,13] We found that **7−9** individually undergo self-assembly in CDCl₃ to yield homodimeric assemblies **8₂** and **9₂** and heterochiral homodimer (+)-**7**·(−)-**7** (Figure 2b) driven by π−π interactions and H-bonds. We found that the three-component mixture **7−9** undergoes high fidelity self-sorting because the hypothetical heterodimers cannot satisfy the geometrical constraints of π−π interactions and simultaneously maximize the number of H-bonds formed.

The results with **7−9** lead us to question whether self-sorting was exceptional behavior or whether the wide variety of H-bonded aggregates known in the literature could simply be mixed together to generate a multicomponent self-sorting system. For this purpose, we selected ten components (**7**, **8**, **10−16**, and barium picrate), which are the components of Davis' self-assembled ionophores, Reinhoudt's rosettes, Rebek's tennis ball and calixarene tetraurea capsule, Meijer's ureidopyrimidinone, and our molecular clips.[14] We found that the ¹H NMR spectrum of the 10-component mixture (Figure 3I) was simply equal to the sum of the NMR spectra of its individual self-assembled species (Figure 3A−H), which is the spectroscopic earmark of a self-sorting system. These studies suggested that simply selecting components with different H-bond donor/acceptor patterns and spatial orientations whose aggregates feature closed networks of H-bonds would enable the preparation of complex self-sorting systems. This work lead supramolecular chemists to appreciate that the subset of molecular aggregates that are capable of self-sorting was much larger than previously appreciated, which inspired numerous research groups to design and study self-sorting systems.

## SELF-SORTING AND STIMULI RESPONSIVE SYSTEMS BASED ON CB[n]-TYPE RECEPTORS

This section details our use of CB[n]-type molecular containers as prime components for the construction of stimuli responsive (self-sorting) systems including those that display allostery, pH and conformational responsiveness, regulation of enzymatic activity, and regulation of in vitro and in vivo biological activity. As discussed, CB[n] compounds are prime components for
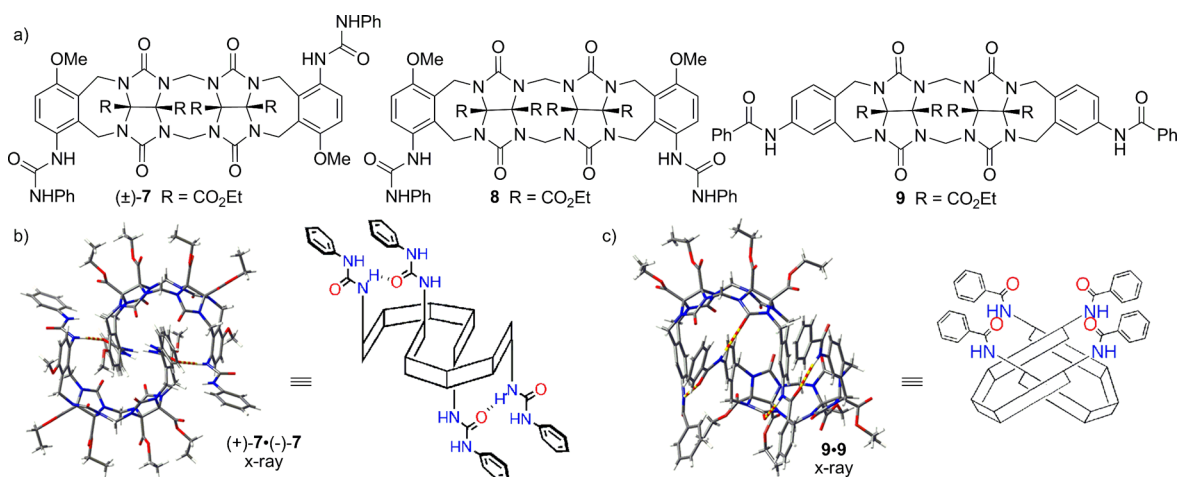
**Figure 2.** Chemical and X-ray structures of self-sorting molecular clips.
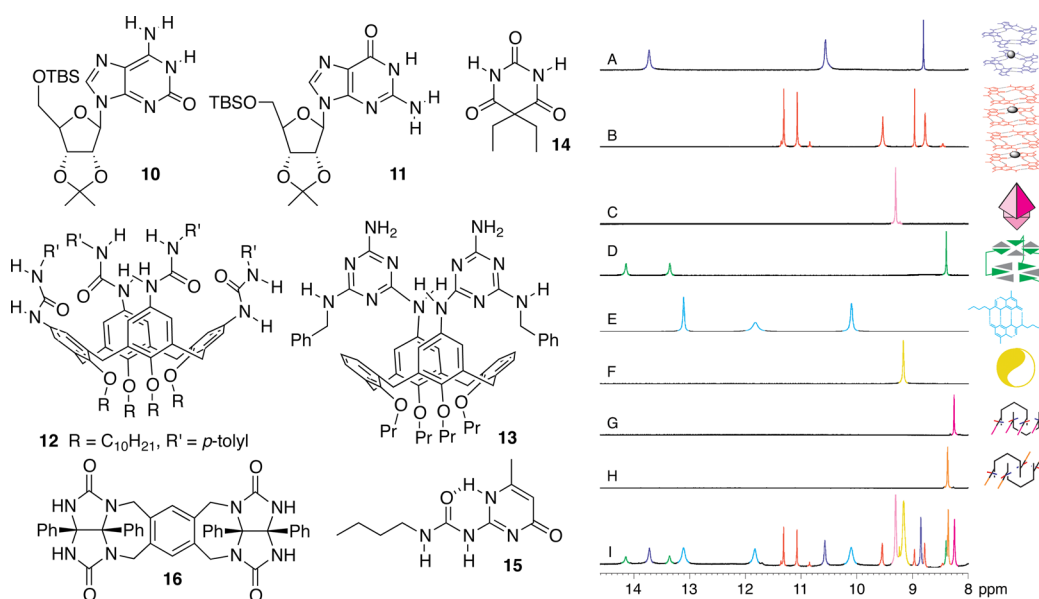


**Figure 3.** Ten-component self-sorting system.

self-sorting systems because of their high affinity and high selectivity interactions, which commonly display slow kinetics of exchange on the chemical shift time scale, which allows for convenient monitoring of the constitution of the mixture by $^1$H NMR spectroscopy.

## Social Self-Sorting

The self-sorting systems discussed above are based on H-bond driven self-recognition processes in CDCl$_3$ where two or more identical molecules self-assemble. We envisioned that self-sorting processes in water based on host–guest complexation events, *social self-sorting*, would be both more biologically relevant and stimuli responsive since addition of exogenous guest could trigger transformation from one self-sorted state to another. For our initial demonstration of social self-sorting, we selected several host–guest pairs (CB[6]·$6_{n=6}$, CB[8]·$17$·$18$, β-cyclodextrin·$19$, and $20$·K$^+$) and other aggregates ($21_2$ and $22_2$·$23_2$) and asked whether their components would faithfully reform these aggregates upon mixing or whether alternate host–guest processes would impinge on the self-sorting process (Figure 4).[15] We found that the $^1$H NMR spectrum of the 12-component mixture is a superposition of the spectra of the six

complexes listed above, which means that this mixture is self-sorted. This work showed that self-sorting proceeds efficiently even in biologically relevant H$_2$O as a medium using inherently less directional electrostatic interactions and the hydrophobic effect. Furthermore, the high fidelity self-sorting suggested to us that the high affinity and selectivity observed for CB[6][16] would also be observed for CB[$n$] homologues.

## CB[$n$] Exhibit High Affinity and High Selectivity Host–Guest Interactions

The social self-sorting process described above prompted us to determine the binding constants of CB[7] and CB[8] toward numerous guests by $^1$H NMR competition experiments referenced to absolute $K_a$ values determined by direct UV/vis titrations.[17] Figure 5a shows a selection of the $K_a$ values determined. For example, we discovered that CB[7] exhibits picomolar binding affinity toward adamantaneammonium and ferrocene ammonium ions, **24** and **25**, in 50 mM NaOAc buffered D$_2$O;[17] the high binding affinity of CB[7]·**25** was subsequently confirmed by ITC competition experiments performed by Inoue, Kim, and Kaifer.[18] Equally interesting was the fact that the CB[8]·**24** complex is more than 5000-fold
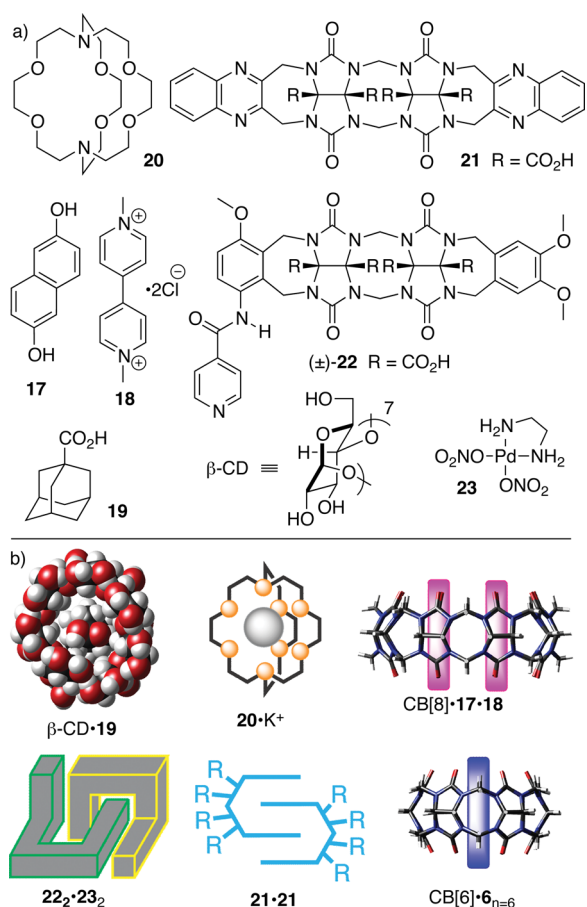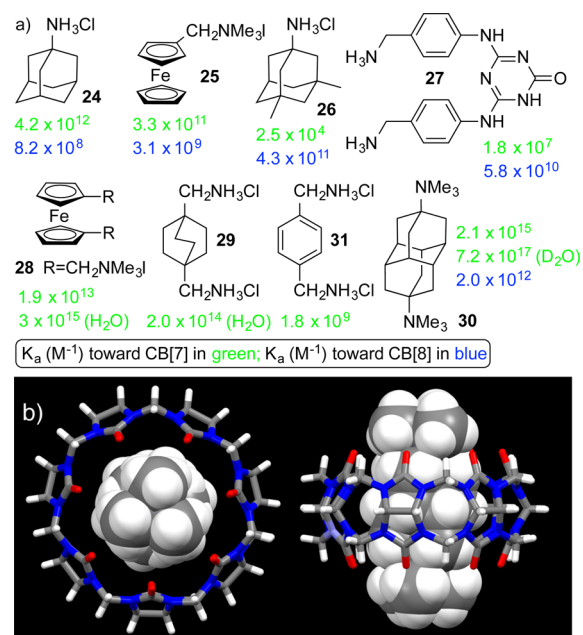
**Figure 4.** Social self-sorting in water.



**Figure 5.** (a) $K_a$ values for selected CB[7] and CB[8] complexes determined in 50 mM NaOAc buffer and (b) X-ray structure of CB[7]·**30**.

weaker than CB[7]·**24**. Conversely, the CB[8]·**26** complex is more than $10^7$-fold tighter than CB[7]·**26**. Similar to many protein–ligand complexes, the addition of Me-groups greatly

destabilizes the CB[7]·**26** complex due to unfavorable steric interactions between the convex surface of the guest and the concave surface of the host. Recent work by Scherman, DeSimone, and Nau suggests that an important factor in the high affinity binding of CB[n] is the release of high energy waters from the CB[n] cavity upon complexation.[19] We also measured the $K_a$ values between guest **27** (available from a concurrent study)[8] and CB[7] and CB[8]; the encapsulation of both ammonium arms within CB[8]·**27** leads to 3200-fold higher affinity and conformational control. Intrigued by the high affinity binding of CB[7]·**24**, several groups sought to reach even higher levels of affinity. In 2007, a collaboration between the Inoue, Kim, Kaifer, Gilson, and Isaacs groups studied the CB[7]·**28** complex in pure water and measured $K_a$ = 3 × $10^{15}$ $M^{-1}$, which is comparable to that of avidin–biotin;[20] the ability of **28** to engage in ion–dipole interactions with both C=O portals was deemed of critical importance. Additional ferrocene and [2.2.2]bicyclooctane diammonium ions (**29**) have been explored in this context.[21,22] Recently, the Glaser–Majerski–Isaacs team reported that diamantanediammonium ion **30** forms CB[7]·**30** with $K_d$ = 1.4 aM![23] This remarkable result was attributed to the presence of 14 optimal ion–dipole interactions, the colinearity of the symmetry axes of CB[7] and **30** within CB[7]·**30**, and the greater hydrophobicity of diamantane relative to adamantane or ferrocene skeletons based on X-ray crystallographic results (Figure 5b).

### Control over Allosteric Processes with CB[n]

In 2005, we reported that addition of guest **27** to CB[10]·CB[5] gave CB[10]·**27**$_2$, which upon reaction with Ac$_2$O followed by washing delivered free CB[10].[8] In searching for guests to fill the voluminous (870 Å$^3$) cavity of CB[10], we found that tetracationic calixarene **32** forms the CB[10]·1,3-*alt*-**32** complex in which **32** preferentially assumes the less stable 1,3-alternate conformation (Scheme 3). Quite interestingly, we found that addition of adamantane derivative **19** resulted in the formation of the CB[10]·cone-**32**·**19**, which amounts to a stimuli responsive conformational control of **32** within the macromolecular complex. Cationic adamantane **24** was much less efficient a stimulus than **19** presumably due to unfavorable electrostatic interactions in the CB[10]·cone-**32**·**14** ternary complex. To reverse the conformational change, we added CB[7] as a stimulus, which sequesters **19** as its CB[7]·**19** complex. The formation of CB[7]·**19** ($K_a$ = 3.2 × $10^8$ $M^{-1}$) provides the free energy needed to drive the conformational change. In this manner, alternate addition of **19** and CB[7] can be used as chemical stimuli to exert allosteric control over the conformation of calixarene **32**.

### Size Dependent Homotropic Allostery with Bis-*nor-seco*-CB[10]

During our studies of the mechanism of CB[n] formation, we isolated bis-*ns*-CB[10], which is formed by step-growth polymerization.[24] Bis-*ns*-CB[10] features two cavities, each shaped by five glycolurils and connected by one CH$_2$–bridge (Figure 6). Bis-*ns*-CB[10] forms ternary complexes with a variety of guest molecules including **24**, **31**, **33**, and **34**. Molecular modeling shows that the cavity volume (450 to 740 Å$^3$) and H$_2$C···CH$_2$ nonbonded distance (5.5 to 9.3 Å) increase systematically as the size of the included guest increases. Therefore, we hypothesized that the binding of the first guest to give bis-*ns*-CB[10]·guest complexes would change the size of the second cavity (Figure 6c). Further, we suspected that the second cavity would display a preference to bind a guest of

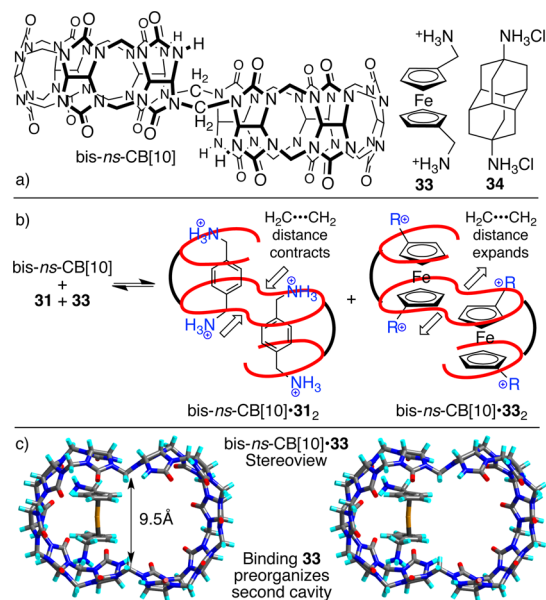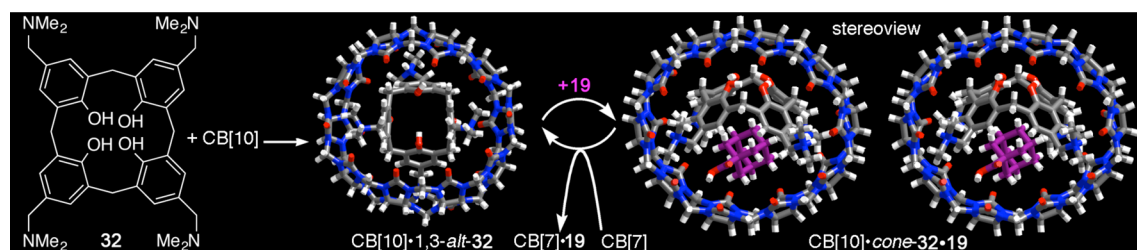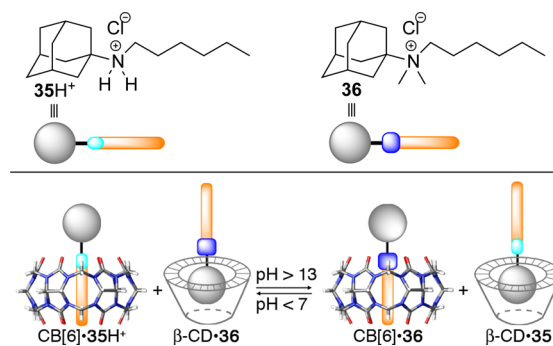**Scheme 3. Conformational Responsiveness of 32 within CB[10]**





**Figure 6.** Size dependent homotropic allostery with bis-*ns*-CB[10].
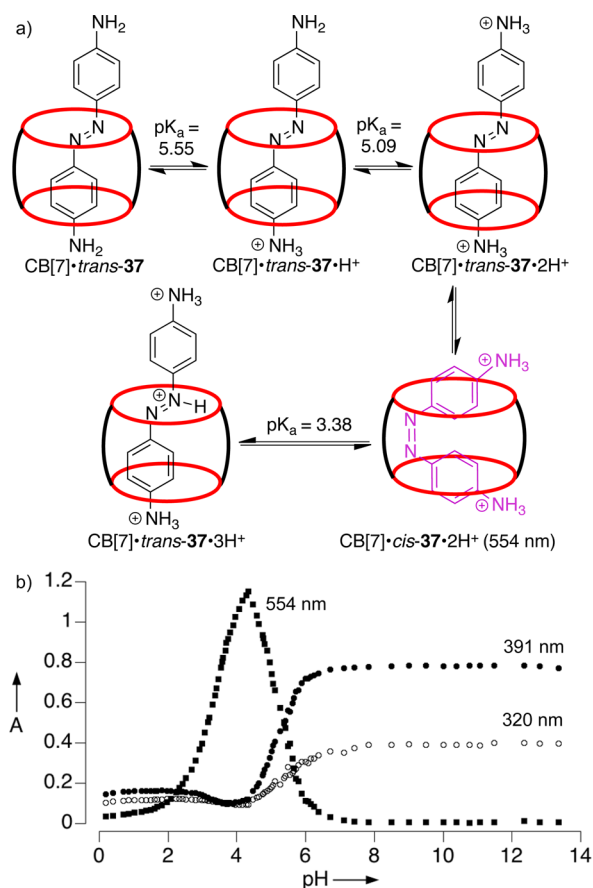
**Scheme 4. Four Component Guest Swapping Ensemble**



(89%) at pH 13 are CB[6]·**36** and $\beta$-CD·**35** as monitored by $^1$H NMR spectroscopy. Thermodynamic calculations using Gepasi show that the magnitude of the p$K_a$ shift (e.g., $\Delta\Delta G$) between CB[6]·**35**H$^+$ and **35**H$^+$ is the critical parameter governing the guest swapping process.

**Azobenzene Cis−Trans Isomerization**

A more complex pH responsive system comprises CB[7] and azobenzene derivative **37** (Scheme 5a).[26] Azobenzene derivatives typically prefer the *trans*-form over the *cis*-form by approximately 10 kcal mol$^{-1}$. However, when we mixed CB[7] with **37** (D$_2$O, pH 4.74), we observed the purple color that is typical of *cis*-azobenzenes. We performed a pH titration (pH 0.5 to 12.5) of **37** alone and did not observe any purple color; the three p$K_a$ values of **37**·H$^+$ (3.54), **37**·2H$^{2+}$ (2.11), and **37**·3H$^{3+}$ (−0.5) agreed with previous literature reports. Subsequently, we performed a UV/vis titration for the CB[7]·**37** complex from pH 0.17 to 13.35. Plots of absorbance (320, 554, and 391 nm) as a function of pH allowed us to extract three p$K_a$ values for the CB[7]·**37**·H$^+$ (5.55), CB[7]·**37**·2H$^{2+}$ (5.09), and CB[7]·**37**·3H$^{3+}$ (3.38) complexes (Scheme 5b). The magnitude of the p$K_a$ shifts induced upon CB[7] binding for **37**·3H$^{3+}$ and **37**·2H$^{2+}$ are quite substantial and approach the magnitude of shifts observed by Nau[27] and Raymond[28] for other container complexes. Quite interestingly, decreasing the pH (7 to 5) results in the formation of CB[7]·*trans*-**37**·H$^+$ and then CB[7]·*trans*-**37**·2H$^{2+}$, which undergoes *thermal* isomerization to the CB[7]·*cis*-**37**·2H$^{2+}$ complex (Scheme 5a). We suggest that the very high $K_a$ values typically observed for CB[7] complexes and the better match of *cis*-**37**·2H$^{2+}$ than *trans*-**37**·2H$^{2+}$ toward the hydrophobic cavity and electrostatically negative C=O portals of CB[7] provide the potent thermodynamic driving force to overcome the 10 kcal mol$^{-1}$ preference for *trans*-azobenzenes. Decreasing pH below 3.4 results in *cis*-to-*trans* isomerization to yield CB[7]·*trans*-**37**·3H$^{3+}$. We used this highly pH responsive UV/vis active system to construct indicator displacement assays for acetylcholine, caffeine, nicotine, dopamine, L-adrenaline, ephedrine, and

similar size by homotropic allostery. To test this hypothesis, we prepared mixtures comprising bis-*ns*-CB[10] and pairs of guests (e.g., **31** + **33**; **24** + **34**) and monitored the process by $^1$H NMR spectroscopy. We observed that mixtures of small and large guests (e.g., **31** + **33**) do indeed undergo size dependent homotropic allostery to yield bis-*ns*-CB[10]·**31**$_2$ and bis-*ns*-CB[10]·**33**$_2$; whereas guests of comparable size (**24** + **34**) form mixtures of the two homomeric and the heteromeric ternary complex bis-*ns*-CB[10]·**24**·**34**. The binding of the first guest acts as a stimulus, which instructs the second binding site to assume a specific size.

**pH Controlled Guest Swapping**

CB[*n*] compounds bind substantially tighter to cationic guests (**GH**$^+$) than to the corresponding neutral form (**G**), which is reflected in a p$K_a$ shift within the CB[*n*]·**GH**$^+$ complex. We designed a four component system comprising two guests and two hosts to undergo controlled guest swapping in response to a change in pH (Scheme 4).[25] As the hosts, we selected $\beta$-cyclodextrin ($\beta$-CD), which is not selective based on guest charge, and CB[6], which is highly selective for cationic over neutral guests. We selected guest **35**H$^+$, which is pH sensitive, and guest **36**, which remains cationic over the full pH range. Guests **35**H$^+$ and **36** contain adamantaneammonium binding epitopes to promote binding toward $\beta$-CD and hexylammonium tails to promote CB[6] binding. At pH 7, an equimolar mixture of all four components mainly forms CB[6]·**35**H$^+$ and $\beta$-CD·**36** (84%). At pH 13, **35**H$^+$ becomes deprotonated to **35**, whereas **36** remains cationic. Accordingly, the dominant species

**Scheme 5. Equilibria in the System Comprising CB[7] and 37**



**a)**

CB[7]·*trans*-37    $pK_a = 5.55$    CB[7]·*trans*-37·H⁺    $pK_a = 5.09$    CB[7]·*trans*-37·2H⁺

CB[7]·*trans*-37·3H⁺    $pK_a = 3.38$    CB[7]·*cis*-37·2H⁺ (554 nm)

**b)**



direction and magnitude of changes in chemical shift upon complexation, we established that two CB[7] bind to the terminal benzylammonium rings of **38** to give CB[7]·a,s,s,a-**38**·CB[7], whereas CB[8] forms the CB[8]·a,a,a,s-**38**, and CB[10] forms the CB[10]·a,a,a,a-**38** complex. We envisioned that we could fold, unfold, and refold a single oligomer strand in response to chemical stimuli. Initially, **38** populates the full 10-component conformational ensemble. However, upon addition of CB[8], the CB[8]·a,a,a,s-**38** conformation is selectively stabilized. Addition of 2 equiv of CB[7] and **26** results in ejection and unfolding of **38** followed by the refolding into the CB[7]·a,s,s,a-**38**·CB[7] conformation. The formation of the CB[8]·**26** complex provides the thermodynamic driving force to promote this process. Interestingly, we observed that the addition of 1 equiv of CB[7] enhances the rate of dissociation of the CB[8]·a,a,a,a-**38** by formation of ternary complex CB[8]·a,a,s,s-**38**·CB[7]. Finally, the addition of 2 equiv of **24** and CB[10]·CB[5] results in the expulsion and forced unfolding of **38** into free solution where it displaces CB[5] and folds to form CB[10]·a,a,a,a-**38** driven by the free energy of formation of the CB[7]·**24** complex. The work is reminiscent of chaperone proteins, which forcibly unfold misfolded proteins and provide an environment for the refolding.

In 2009, we isolated acyclic glycoluril decamer (±)-**39** in racemic form.[30] When dissolved in water, (±)-**39** exhibits a poorly resolved ¹H NMR spectrum indicative of a range of conformations around the central N−CH₂−N bridge. Quite interestingly, addition of metal sulfate salts (100 mM Li⁺, Na⁺, K⁺, or Ca²⁺) triggers folding and heterochiral dimerization processes to yield (+)-**39**·(−)-**39**·6Na⁺ driven by strong ion−dipole interactions between three or four C=O groups and each of the Na⁺ ions. The X-ray crystal structure of (+)-**39**·(−)-**39**·6Na⁺ is shown in Scheme 7. It is possible to reverse this folding and heterochiral dimerization process by the addition of **31**, which gives the (±)-**39**·**31**₂ complex; subsequent addition of CB[7] sequesters **31** as the CB[7]·**31** complex and results in the reformation of the (+)-**39**·(−)-**39**·6Na⁺ complex. These processes amount to a metal ion responsive folding and assembly process that is reminiscent of RNA folding processes. CB[n] containers are privileged in that they display protein mimetic (e.g., tight and selective binding) and nucleic acid mimetic (e.g., metal ion responsive) processes.

Recently, we reported the preparation of CB[6] dimer **40** by the reaction of glycoluril hexamer with 1,2,4,5-tetraformylbenzene.[31] Compound **40** (3 equiv) undergoes self-assembly with oligomer **41** (2 equiv) to yield supramolecular ladder **40**₃·**41**₂ as shown in Scheme 8 as established by ¹H NMR symmetry

pseudoephedrine and were able to quantitate pseudoephedrine concentration in the over-the-counter nasal decongestant Sudafed in the 5−350 $\mu$M range.
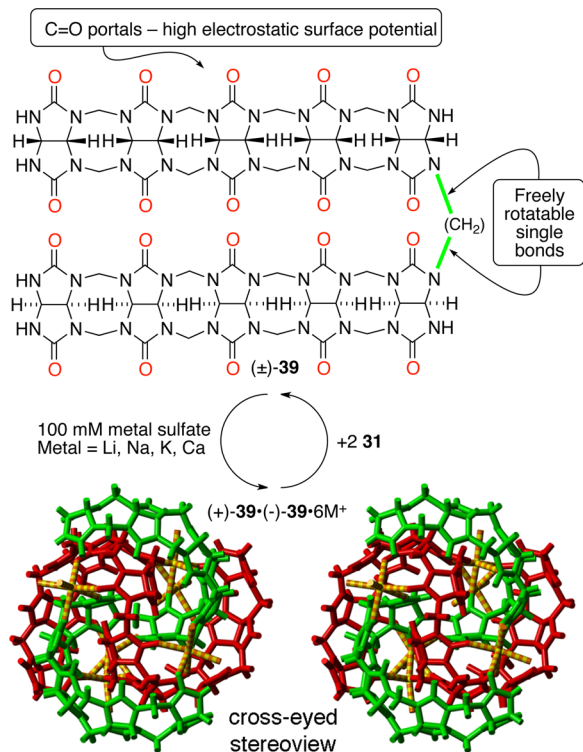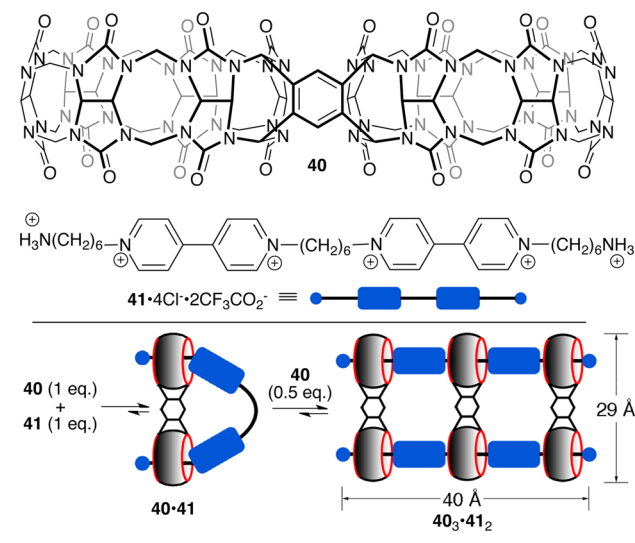
### Controlled Folding Processes

Our earlier experience with the binding of **27** with CB[7], CB[8], and CB[10] prompted us to use CB[n] complexation to control the conformation of longer triazene−arylene oligomer **38** and related structures.[29] By virtue of its four exocyclic triazene−NHAr bonds (green), oligomer **38** populates $2^4$ conformations of which 10 are unique (Scheme 6). We studied the interaction of **38** with CB[7], CB[8], and CB[10] by a combination of ¹H NMR spectroscopy and X-ray crystallography. Based on symmetry arguments and the observed

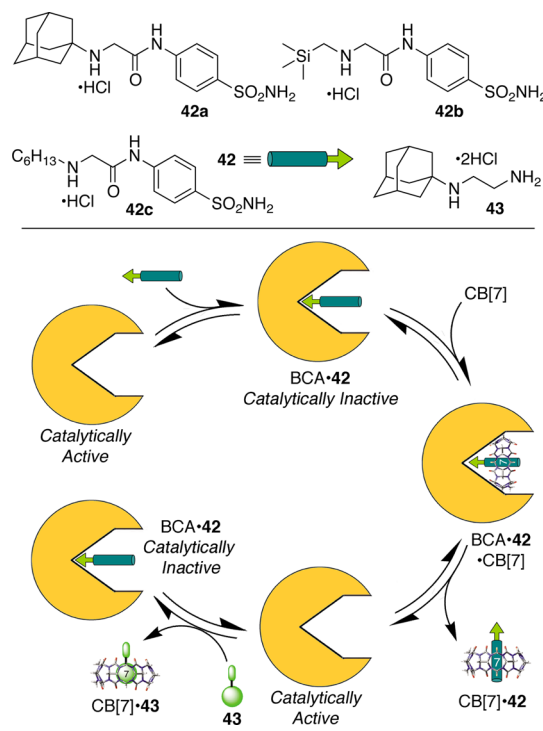**Scheme 6. Folding Oligomer 38 with CB[n] Containers**

## Scheme 7. Folding and Assembly of (±)-39



## Scheme 8. Formation of Supramolecular Ladder $40_3 \cdot 41_2$



considerations and diffusion coefficient measurements (DOSY). Complex $40_3 \cdot 41_2$ is comparable in weight (7389 amu) and dimension ($40 \times 29 \times 11$ Å³) to small proteins. Interestingly, an equimolar mixture of **40** and **41** yields the folded **40·41** assembly wherein the two terminal hexylene binding sites of **41** are complexed to fully satisfy both cavities of **40**. The folded structure of **40·41** was assigned on the basis of complexation induced chemical shifts, symmetry considerations, DOSY, and electrospray ionization mass spectrometry measurements. When more **40** (0.5 equiv) is added, the assembly is transformed into $40_3 \cdot 41_2$ in a process that is responsive to host–guest stoichiometry.

## Control over Enzymatic Catalysis

We envisioned that the extremely high binding constants commonly exhibited by CB[7]−guest complexes could be used to outcompete biological macromolecules for their targets and thereby exert stimuli responsive control over the cognate biological functions. First, we decided to exert control over the catalytic activity of bovine carbonic anhydrase (BCA).[32] We prepared a series of compounds (**42a−c**) that we refer to as two-faced inhibitors that contain a benzenesulfonamide binding epitope, which is well-known to inhibit BCA via binding to the Zn-cofactor at the active site ($K_a \approx 10^7$–$10^8$ M$^{-1}$), and an ammonium ion binding face, which binds to CB[7] (Scheme 9). Compounds **42a−c** contain adamantaneammonium,

## Scheme 9. Control of Enzymatic Activity of BCA



trimethylsilylmethylammonium, and hexylammonium binding epitopes, which possess vastly different $K_a$ values ($\sim 10^{12}$, $10^9$, and $10^6$ M$^{-1}$, respectively) toward CB[7]. Experimentally, we found that addition of **42a−c** to BCA turns off the catalytic ability of BCA as monitored by a standard UV/vis $p$-nitrophenylacetate hydrolysis assay. Addition of CB[7] sequesters **42a** or **42b**, but not **42c**, as their CB[7] complexes and turns on the catalytic activity of BCA. The lower binding affinity of CB[7]·**42c** is insufficient to drive the reactivation of BCA. Similarly, we were unable to reactivate the BCA·**42a** or BCA·**42b** systems by addition of $\beta$-cyclodextrin because of the low $K_a$ values of $\beta$-CD−guest complexes. Subsequent addition of **43** to the BCA + CB[7]·**42b** system competitively displaces two faced inhibitor **42b** from its CB[7]·**42b** complex, which then turns off BCA by formation of BCA·**42b**. We could not regenerate activity of the BCA + CB[7]·**42a** system in this manner because the CB[7]·**42a** complex ($K_a \approx 10^{12}$ M$^{-1}$) exhibits slow dissociation kinetics ($k_{off} \approx 2 \times 10^{-5}$ s$^{-1}$; half-life = 9 h) on the time scale of the experiment. Alternate addition of CB[7] and **43** was able to control enzymatic catalysis of BCA over four on−off cycles. Very interestingly, we found that
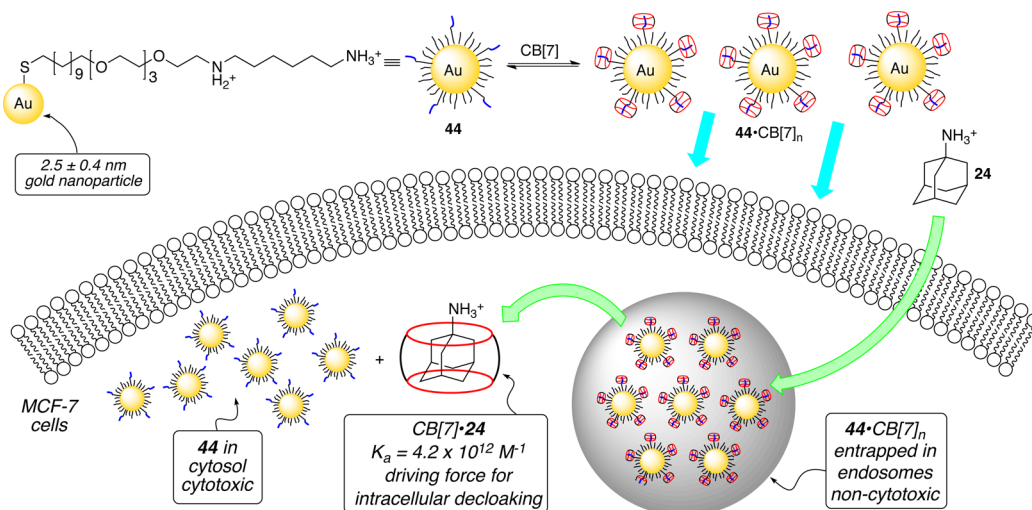
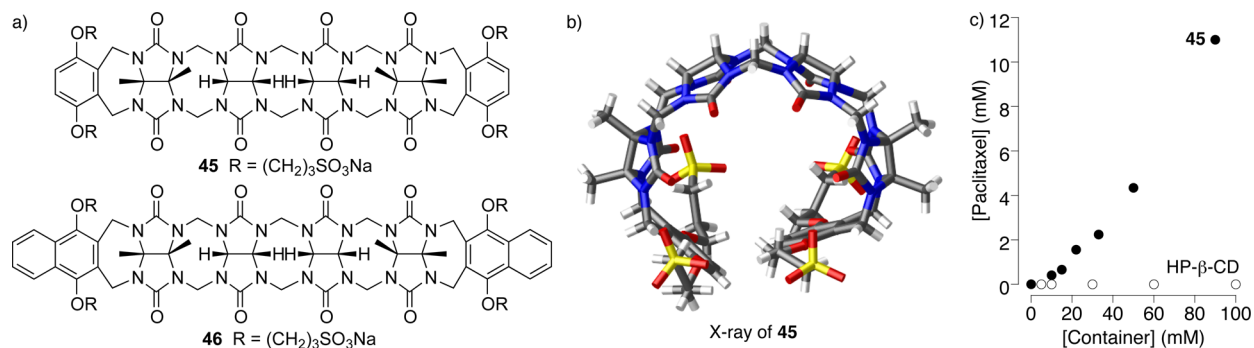**Figure 7.** Intracellular activation of nanoparticle therapeutics.



**Figure 8.** Acyclic CB[$n$] solubilizing containers.

CB[7] enhances the rate of dissociation of BCA·**42a** (11-fold) and BCA·**42b** (19-fold) due to the formation of a transient ternary complex (BCA·**42**·CB[7]). We independently confirmed that the CB[7]·**42a** and CB[7]·**42b** complexes are ~100-fold weaker inhibitors ($K_a \approx 10^5$–$10^6$ M$^{-1}$) of BCA than **42a** or **42b** presumably due to steric interactions between the convex surface of CB[7] and the active site of BCA. The work suggests a path toward stimuli responsive control of protein function in biological systems.

### Control over *in Vitro* Biological Systems

In collaboration with the Rotello group, we sought to use the high affinity and highly selective binding interactions of CB[7] to activate nanoparticle therapeutics intracellularly in a stimuli responsive manner.[33] For this purpose, gold nanoparticles (2.5 ± 0.4 nm diameter) were decorated with hexanediammonium ion terminated alkanethiolates. The terminal hexanediammonium ions renders nanoparticles **44** cytotoxic and also serves as a recognition site for CB[7] (Figure 7). We envisioned that the CB[7] complexed nanoparticle **44**·CB[7]$_n$ would cloak the cytotoxic hexanediammonium ion units and reduce cytotoxicity toward MCF-7 cells. This prediction was borne out experimentally, and one reason for the reduced cytotoxicity was the fact that the **44**·CB[7]$_n$ nanoparticles become entrapped in endosomes. Furthermore, we found that the addition of **24** to MCF-7 cells that had already been treated with **44**·CB[7]$_n$ sequesters CB[7] from the nanoparticle surface driven by the free energy of formation of CB[7]·**24**. This process triggers the release of the naked nanoparticle **44** from

the endosome and results in higher levels of cytotoxicity. The ability to intracellularly activate nanoparticle therapeutics triggered by **24** offers potential routes to dual (e.g., host and guest) targeted therapeutics with higher levels of site-specific activity.

Recently, we have been studying the preparation and molecular recognition properties of acyclic CB[$n$]-type molecular containers **45** and **46** (Figure 8a).[34] Compounds **45** and **46** feature a central glycoluril tetramer, two terminal aromatic rings, and four SO$_3^-$ groups, which dramatically enhance their solubility in water. Compounds **45** and **46** are preorganized into a C-shaped conformation (Figure 8b) and are not significantly self-associated in water. Significantly, the acyclic nature of **45** and **46** and the flexibility of the glycoluril tetramer backbone allow these compounds to flex like a hand to accommodate a wide range of guest sizes. We found that **45** and **46** greatly enhance the water solubility (from 23-fold to 2750-fold) of a number of insoluble drugs (e.g., paclitaxel, melphalan, clopidogrel, amiodarone, and camptothecin, Figure 8c). Acyclic CB[$n$]-type container **45** does not display significant *in vitro* toxicity toward kidney (HepG2), liver (HEK 293), and human monocyte (THP-1) cells according to metabolic cell viability and adenylate kinase release cell death assays. The *in vivo* (Swiss Webster mice) maximum tolerated dose (MTD) studies with **45** indicated an MTD greater than 1.23 g kg$^{-1}$. Treatment of HeLa cells with paclitaxel solubilized with **45** results in enhanced cell killing relative to the paclitaxel alone. This study establishes proof-of-principle for use of

acyclic CB[*n*]-type containers for drug solubilization and delivery. These *in vitro* studies rely on drug displacement by competitive binding of **45** toward endogenous compounds whereas the corresponding *in vivo* application of cyclodextrin·drug complexes also benefits from the dilution of the container·drug complex from above to below $K_d$.

Recently, the Isaacs group discovered the templated synthesis of methylene bridged glycoluril hexamer, which can be transformed into monofunctionalized CB[7] derivatives by reaction with glycoluril bis(cyclic ethers).[35] We adapted this chemistry to prepare CB[7] derivative **47**, which bears a covalently attached biotin ligand on its convex surface.[36] Container **47** is capable of forming complexes with chemotherapeutic agents (oxaliplatin, camtothecin, tamoxifen, temezolomide, albendazole, or irinotecan). We monitored the internalization of the fluorescent complexes **47·48** and CB[7]·**48** into murine lymphocytic leukemia cells (L1210) and their derived cell line L1210FR, which overexpresses biotin receptors, by confocal microscopy and flow cytometry (Figure 9). These experiments indicated enhanced uptake of **47·48** by a
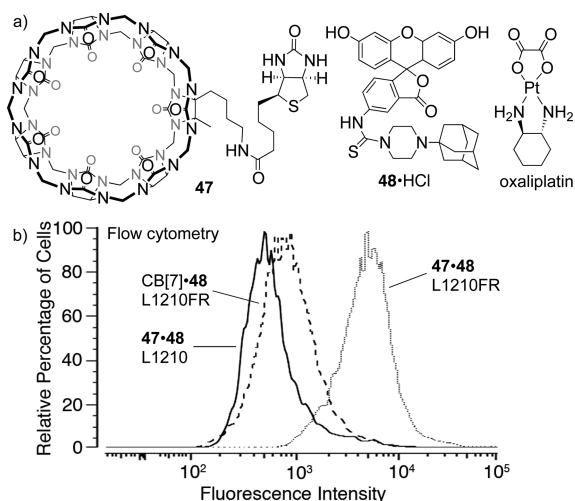


**Figure 9.** *In vitro* targeting of **47**·oxaliplatin.

receptor mediated endocytosis pathway. Subsequently, we monitored the cell viability of L1210 and L1210FR cells after treatment with targeted **47**·oxaliplatin versus untargeted CB[7]·oxaliplatin. We observed an approximate 10-fold decrease in EC$_{50}$ for **47**·oxaliplatin relative to CB[7]·oxaliplatin. This work opens the door toward the use of CB[*n*] derivatives for the targeted delivery of drugs to specific locations *in vivo*.

## Control over *in Vivo* Biological Systems

Similar to the cyclodextrins, the *in vitro* applications of acyclic CB[*n*]-type containers rely on their comparably weak binding toward many drugs, which allows for release upon competitive displacement or dilution. Sugammadex is a γ-cyclodextrin derivative that binds tightly to the neuromuscular blocking agents rocuronium and vecuronium ($K_a \approx 10^7$ M$^{-1}$).[37] Sugammadex is marketed by Merck under the trade name Bridion in Europe for the clinical reversal of neuromuscular block induced by rocuronium and vecuronium but has not yet been approved by the US FDA.[37] We envisioned that acyclic CB[*n*]-type containers **45** and **46** would bind strongly to rocuronium, vecuronium, and *cis*-atracurium because they are hydrophobic steroidal dications (Figure 10a).[38] Using a combination of direct UV/vis titrations and competition assays
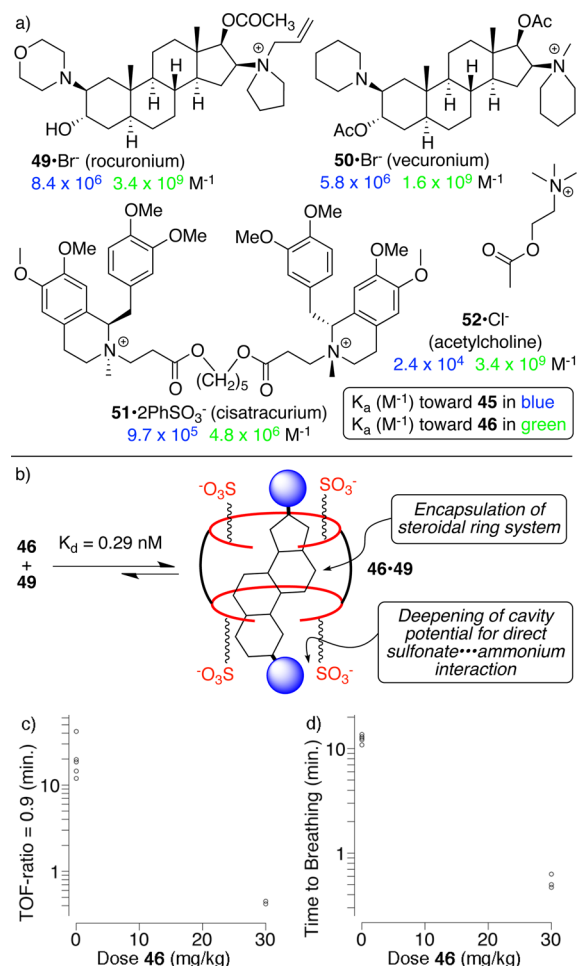


**Figure 10.** Binding of NMBAs by **45** and **46** *in vitro* and reversal of neuromuscular block *in vivo* in rats.

allowed us to measure the $K_a$ values for **45** and **46** toward neuromuscular blocking agents **49**−**51** and acetylcholine **52**. The affinity of **46** toward rocuronium is 300-fold higher than that of sugammadex[37] and is 19000-fold selective for rocuronium over acetylcholine **52**, which prompted us to perform *in vivo* reversal experiments (Figure 10c). Experimentally, rats were anesthetized with isofluorane, and their neuromuscular function was blocked by administration of rocuronium (3.5 mg kg$^{-1}$). Subsequent treatment with **46** (30 mg kg$^{-1}$) resulted in a rapid reversal of neuromuscular block as evidenced by the dramatic decrease in time required for spontaneous breathing and a return to a train-of-four (TOF) ratio of 0.9. Related experiments conducted using **45** demonstrate the reversal of neuromuscular block induced by rocuronium and also *cis*-atracurium, which has not been demonstrated for sugammadex.[39] Treatment with **45** (≤150 mg kg$^{-1}$) does not result in changes in heart rate, mean arterial pressure, or blood chemistry (pH, pO$_2$, or pCO$_2$). Further development of **45** and particularly **46** as broad spectrum reversal agents for neuromuscular block is in progress.

## ■ CONCLUDING REMARKS

CB[*n*] and CB[*n*]-type receptors display remarkably high affinity toward their target guests in water as exemplified by the CB[7]·**30** complex with $K_d$ = 1.4 aM. Furthermore, CB[*n*]-type receptors are quite selective in that different hosts display quite

2060

dx.doi.org/10.1021/ar500075g | *Acc. Chem. Res.* 2014, 47, 2052−2062

different affinity toward a common guest and conversely that a given host is quite selective among a pool of guests. Accordingly, CB[n]−guest derived systems are inherently stimuli responsive (e.g., pH, photochemical, electrochemical, chemical). In this Account, we presented the progression of our work in this area beginning with self-sorted H-bonded molecular clips and collections of H-bonded aggregates by self-association processes and continuing to the development of stimuli responsive systems based on the extremely high affinity ($K_a$ up to $10^{17}$ $M^{-1}$) and selectivity displayed by CB[n]-type containers toward their guests, which provides the free energy driving force to reconfigure multicomponent systems. For example, we constructed systems that display size-dependent homotropic allostery, controlled folding−unfolding−refolding transitions of a triazene−arylene oligomer, pH triggered guest swapping, pH promoted azobenzene trans−cis isomerization, and control over enzymatic activity of BCA. In the final sections, we showed that CB[n]-type receptors could be used to express control over biological systems both in vitro and in vivo. For example, CB[7] can be used to cloak the toxicity of gold nanoparticles **44**, which can be decloaked by addition of **24** inside MCF-7 cells, biotin-targeted CB[7] **47** enhances the bioactivity of oxaliplatin toward L1210FR cells 10-fold, and acyclic CB[n]-type receptors **45** and **46** can enhance the solubility and bioactivity of drugs like paclitaxel. Finally, compound **46** binds to rocuronium in vitro and reverses neuromuscular block in vivo in rats. Accordingly, the future prospects for the use of CB[n]-type receptors as stimuli responsive components to trigger reconfiguration of a system between two or more distinct states for both technological and biological applications are extremely bright.

## ■ AUTHOR INFORMATION

### Corresponding Author

*Phone: 301-405-1884. Fax: 301-314-9121. E-mail: LIsaacs@umd.edu.

### Notes

The authors declare no competing financial interest.

### Biography

**Lyle Isaacs** was born in New York City in 1969 and was educated at the Bronx High School of Science, University of Chicago (B.S. 1991), University of California (M.S. 1992), and Swiss Federal Institute of Technology (Zürich), where he received his doctoral degree under the guidance of Prof. Francois Diederich in 1995. After an NIH postdoctoral fellowship with Prof. George Whitesides at Harvard, he started his independent career at the University of Maryland in 1998 and is currently Professor of Chemistry. The Isaacs group uses its knowledge of the fundamental molecular recognition properties and mechanism of CB[n] formation to create new CB[n]-type receptors for biomimetic and drug delivery applications.

## ■ ACKNOWLEDGMENTS

## ■ REFERENCES

(1) Kramer, R.; Lehn, J.-M.; Marquis-Rigault, A. Self-Recognition in Helicate Self-Assembly: Spontaneous Formation of Helical Metal Complexes from Mixtures of Ligands and Metal Ions. *Proc. Natl. Acad. Sci. U.S.A.* **1993**, *90*, 5394−5398.

(2) Rowan, S. J.; Hamilton, D. G.; Brady, P. A.; Sanders, J. K. M. Automated Recognition, Sorting, and Covalent Self-Assembly by Predisposed Building Blocks in a Mixture. *J. Am. Chem. Soc.* **1997**, *119*, 2578−2579.

(3) Freeman, W. A.; Mock, W. L.; Shih, N.-Y. Cucurbituril. *J. Am. Chem. Soc.* **1981**, *103*, 7367−7368.

(4) Rowan, A. E.; Elemans, J. A. A. W.; Nolte, R. J. M. Molecular and Supramolecular Objects from Glycoluril. *Acc. Chem. Res.* **1999**, *32*, 995−1006.

(5) Rebek, J., Jr. Reversible Encapsulation and Its Consequences in Solution. *Acc. Chem. Res.* **1999**, *32*, 278−286.

(6) Kim, J.; Jung, I.-S.; Kim, S.-Y.; Lee, E.; Kang, J.-K.; Sakamoto, S.; Yamaguchi, K.; Kim, K. New Cucurbituril Homologues: Syntheses, Isolation, Characterization, and X-ray Crystal Structures of Cucurbit-[n]uril (n = 5, 7, and 8). *J. Am. Chem. Soc.* **2000**, *122*, 540−541.

(7) Day, A.; Arnold, A. P.; Blanch, R. J.; Snushall, B. Controlling Factors in the Synthesis of Cucurbituril and Its Homologues. *J. Org. Chem.* **2001**, *66*, 8094−8100.

(8) Liu, S.; Zavalij, P. Y.; Isaacs, L. Cucurbit[10]uril. *J. Am. Chem. Soc.* **2005**, *127*, 16798−16799.

(9) Masson, E.; Ling, X.; Joseph, R.; Kyeremeh-Mensah, L.; Lu, X. Cucurbituril Chemistry: A Tale of Supramolecular Success. *RSC Adv.* **2012**, *2*, 1213−1247.

(10) Isaacs, L. The Mechanism of Cucurbituril Formation. *Isr. J. Chem.* **2011**, *51*, 578−591.

(11) Lucas, D.; Minami, T.; Iannuzzi, G.; Cao, L.; Wittenberg, J. B.; Anzenbacher, P.; Isaacs, L. Templated Synthesis of Glycoluril Hexamer and Monofunctionalized Cucurbit[6]uril Derivatives. *J. Am. Chem. Soc.* **2011**, *133*, 17966−17976.

(12) Wu, A.; Chakraborty, A.; Fettinger, J. C.; Flowers, R. A., II; Isaacs, L. Molecular clips that undergo heterochiral aggregation and self-sorting. *Angew. Chem., Int. Ed.* **2002**, *41*, 4028−4031.

(13) Ghosh, S.; Wu, A.; Fettinger, J. C.; Zavalij, P. Y.; Isaacs, L. Self-Sorting Molecular Clips. *J. Org. Chem.* **2008**, *73*, 5915−5925.

(14) Wu, A.; Isaacs, L. Self-Sorting: The Exception or the Rule? *J. Am. Chem. Soc.* **2003**, *125*, 4831−4835.

(15) Mukhopadhyay, P.; Wu, A.; Isaacs, L. Social Self-Sorting in Aqueous Solution. *J. Org. Chem.* **2004**, *69*, 6157−6164.

(16) Mock, W. L.; Shih, N. Y. Structure and Selectivity in Host−Guest Complexes of Cucurbituril. *J. Org. Chem.* **1986**, *51*, 4440−4446.

(17) Liu, S.; Ruspic, C.; Mukhopadhyay, P.; Chakrabarti, S.; Zavalij, P. Y.; Isaacs, L. The Cucurbit[n]uril Family: Prime Components for Self-Sorting Systems. *J. Am. Chem. Soc.* **2005**, *127*, 15959−15967.

(18) Jeon, W. S.; Moon, K.; Park, S. H.; Chun, H.; Ko, Y. H.; Lee, J. Y.; Lee, E. S.; Samal, S.; Selvapalam, N.; Rekharsky, M. V.; Sindelar, V.; Sobransingh, D.; Inoue, Y.; Kaifer, A. E.; Kim, K. Complexation of Ferrocene Derivatives by the Cucurbit[7]uril Host: A Comparative Study of the Cucurbituril and Cyclodextrin Host Families. *J. Am. Chem. Soc.* **2005**, *127*, 12984−12989.

(19) Biedermann, F.; Uzunova, V. D.; Scherman, O. A.; Nau, W. M.; De Simone, A. Release of High-Energy Water as an Essential Driving Force for the High-Affinity Binding of Cucurbit[n]urils. *J. Am. Chem. Soc.* **2012**, *134*, 15318−15323.

(20) Rekharsky, M. V.; Mori, T.; Yang, C.; Ko, Y. H.; Selvapalam, N.; Kim, H.; Sobransingh, D.; Kaifer, A. E.; Liu, S.; Isaacs, L.; Chen, W.; Moghaddam, S.; Gilson, M. K.; Kim, K.; Inoue, Y. A Synthetic Host-Guest System Achieves Avidin-Biotin Affinity by Overcoming Enthalpy-Entropy Compensation. *Proc. Natl. Acad. Sci. U.S.A.* **2007**, *104*, 20737−20742.

(21) Moghaddam, S.; Yang, C.; Rekharsky, M.; Ko, Y. H.; Kim, K.; Inoue, Y.; Gilson, M. K. New Ultrahigh Affinity Host-Guest Complexes of Cucurbit[7]uril with Bicyclo[2.2.2]octane and Adamantane Guests: Thermodynamic Analysis and Evaluation of M2 Affinity Calculations. *J. Am. Chem. Soc.* **2011**, *133*, 3570−3581.

(22) Kaifer, A. E.; Li, W.; Yi, S. Cucurbiturils as Versatile Receptors for Redox Active Substrates. *Isr. J. Chem.* **2011**, *51*, 496−505.

(23) Cao, L.; Sekutor, M.; Zavalij, P. Y.; Mlinaric-Majerski, K.; Glaser, R.; Isaacs, L. Cucurbit[7]uril·Guest Pair with an Attomolar Dissociation Constant. *Angew. Chem., Int. Ed.* **2014**, *53*, 988−993.

(24) Huang, W.-H.; Liu, S.; Zavalij, P. Y.; Isaacs, L. Nor-Seco-Cucurbit[10]uril Exhibits Homotropic Allosterism. *J. Am. Chem. Soc.* **2006**, *128*, 14744−14745.

(25) Chakrabarti, S.; Mukhopadhyay, P.; Lin, S.; Isaacs, L. Reconfigurable Four-Component Molecular Switch Based on pH-Controlled Guest Swapping. *Org. Lett.* **2007**, *9*, 2349−2352.

(26) Wu, J.; Isaacs, L. Cucurbit[7]uril Complexation Drives Thermal trans-cis-Azobenzene Isomerization and Enables Colorimetric Amine Detection. *Chem.—Eur. J.* **2009**, *15*, 11675−11680.

(27) Nau, W. M.; Florea, M.; Assaf, K. I. Deep Inside Cucurbiturils: Physical Properties and Volumes of their Inner Cavity Determine the Hydrophobic Driving Force for Host-Guest Complexation. *Isr. J. Chem.* **2011**, *51*, 559−577.

(28) Pluth, M.; Bergman, R.; Raymond, K. Proton-Mediated Chemistry and Catalysis in a Self-Assembled Supramolecular Host. *Acc. Chem. Res.* **2009**, *42*, 1650−1659.

(29) Liu, S.; Zavalij, P. Y.; Lam, Y.-F.; Isaacs, L. Refolding Foldamers: Triazene-Arylene Oligomers That Change Shape with Chemical Stimuli. *J. Am. Chem. Soc.* **2007**, *129*, 11232−11241.

(30) Huang, W.-H.; Zavalij, P. Y.; Isaacs, L. Metal-Ion-Induced Folding and Dimerization of a Glycoluril Decamer in Water. *Org. Lett.* **2009**, *11*, 3918−3921.

(31) Wittenberg, J. B.; Zavalij, P. Y.; Isaacs, L. Supramolecular Ladders from Dimeric Cucurbit[6]uril. *Angew. Chem., Int. Ed.* **2013**, *52*, 3690−3694.

(32) Ghosh, S.; Isaacs, L. Biological Catalysis Regulated by Cucurbit[7]uril Molecular Containers. *J. Am. Chem. Soc.* **2010**, *132*, 4445−4454.

(33) Kim, C.; Agasti, S. S.; Zhu, Z.; Isaacs, L.; Rotello, V. M. Recognition-Mediated Activation of Therapeutic Gold Nanoparticles Inside Living Cells. *Nat. Chem.* **2010**, *2*, 962−966.

(34) Ma, D.; Hettiarachchi, G.; Nguyen, D.; Zhang, B.; Wittenberg, J. B.; Zavalij, P. Y.; Briken, V.; Isaacs, L. Acyclic Cucurbit[n]uril Molecular Containers Enhance the Solubility and Bioactivity of Poorly Soluble Pharmaceuticals. *Nat. Chem.* **2012**, *4*, 503−510.

(35) Vinciguerra, B.; Cao, L.; Cannon, J. R.; Zavalij, P. Y.; Fenselau, C.; Isaacs, L. Synthesis and Self-Assembly Processes of Monofunctionalized Cucurbit[7]uril. *J. Am. Chem. Soc.* **2012**, *134*, 13133−13140.

(36) Cao, L.; Hettiarachchi, G.; Briken, V.; Isaacs, L. Cucurbit[7]uril Containers for Targeted Delivery of Oxaliplatin to Cancer Cells. *Angew. Chem., Int. Ed.* **2013**, *52*, 12033−12037.

(37) Bom, A.; Bradley, M.; Cameron, K.; Clark, J.; Van Egmond, J.; Feilden, H.; MacLean, E.; Muir, A.; Palin, R.; Rees, D.; Zhang, M.-Q. A Novel Concept of Reversing Neuromuscular Block: Chemical Encapsulation of Rocuronium Bromide by a Cyclodextrin-Based Synthetic Host. *Angew. Chem., Int. Ed.* **2002**, *41*, 266−270.

(38) Ma, D.; Zhang, B.; Hoffmann, U.; Sundrup, M. G.; Eikermann, M.; Isaacs, L. Acyclic Cucurbit[n]uril-Type Molecular Containers Bind Neuromuscular Blocking Agents in Vitro and Reverse Neuromuscular Block in Vivo. *Angew. Chem., Int. Ed.* **2012**, *51*, 11358−11362.

(39) Hoffmann, U.; Grosse-Sundrup, M.; Eikermann-Haerter, K.; Zaremba, S.; Ayata, C.; Zhang, B.; Ma, D.; Isaacs, L.; Eikermann, M. Calabadion: A New Agent to Reverse the Effects of Benzylisoquinoline and Steroidal Neuromuscular-blocking Agents. *Anesthesiology* **2013**, *119*, 317−325.